

Modeling effects of subsurface tension on segregation: Pt₂₅Rh₇₅(111) oscillatory profile used as a test case

Micha Polak* and Leonid Rubinovich

Department of Chemistry, Ben-Gurion University, Beer-Sheva 84105, Israel

(Received 15 March 2006; revised manuscript received 11 July 2006; published 11 January 2007)

Surface induced bond energy variations are incorporated as homoatomic interaction model in the statistical-mechanical free energy concentration expansion method (FCEM) for the prediction of temperature dependent segregation in alloys. This article focuses on the role of subsurface (and outermost) layer tensions in the emergence of oscillatory segregation profiles even in alloys with weak mixing or demixing tendency. As a test case for the proposed approach, surface segregation in Pt₂₅Rh₇₅(111) is computed by FCEM with Naval Research Laboratory (NRL)-tight-binding (TB) data of surface-induced bond energy variations. A distinct two-layer oscillatory profile is obtained in fair agreement with previously reported experimental data. According to TB data, such subsurface bonding effects are anticipated also for some other Pt-based alloys. The FCEM/TB approach can be used also for predicting surface segregation phenomena in alloy nanoclusters.

DOI: [10.1103/PhysRevB.75.045415](https://doi.org/10.1103/PhysRevB.75.045415)

PACS number(s): 68.35.Dv, 05.70.Np, 68.35.Md, 68.47.De

Surface segregation, manifested as a deviation of the surface composition from the bulk value, is very common in metallic alloys. This enrichment in alloy constituent is not limited to the outmost surface layer, where it reaches a maximum, but typically extends either monotonously or oscillatorily to subsurface layers. Such a composition gradient can affect physical and chemical properties relevant to heterogeneous catalysis, oxidation, magnetism, adhesion, etc. The term “surface segregation” usually refers to the free (clean) surface, whereas under gaseous environment chemisorption usually modifies the segregation characteristics. This applies also to Pt-Rh dispersed material that is widely used in the detoxication of car exhaust gases as a “three-way catalyst.” Since the intrinsic and chemical driving forces operate concomitantly, study of free surface segregation forms a basis for the other case. Experimental measurement of layer by layer compositions is quite tedious and is limited to just a few dedicated techniques. This has motivated numerous theoretical computational studies in this field.¹

A combination of statistical mechanics and input energetic parameters is often used for the prediction of surface segregation and related thermodynamic properties in bulk alloys and alloy clusters. A variety of theoretical approaches to the surface energetics have been employed, ranging from simplified empirical bond energies² to *ab initio* density functional theory (DFT).³ Also, semiempirical potentials, such as the embedded atom method (EAM),^{4–6} the effective medium theory (EMT),^{7,8} and the tight-binding (TB) based second moment approximation (SMA) (Refs. 9 and 10) have been used. Electronic structure approaches to surface energetics of transition metals, based on parametrized TB Hamiltonians, were first performed using a scheme based on a pure *d* band model,^{11–13} and later used improved *spd* tight-binding methods (required for cases of almost filled or empty *d* band).¹⁴ Being much less time consuming, TB electronic structure calculations produce results in good agreement with *ab initio* DFT on simple systems, and open up the possibility of studying rough surfaces and clusters.^{15,16} Compared to computer simulations, statistical-mechanical approximations based on analytical expressions for the alloy free energy have some

advantages, such as much higher computing efficiency. In particular, numerical minimization of the free energy with respect to atomic site concentrations readily provides their equilibrium values. In early works, the simple Bragg-Williams (BW) approximation was used,^{17,18} while studies that went beyond it include the Bethe or quasichemical approximation^{19,20} and the cluster variation method (CVM),^{21–24} all reviewed in Ref. 1. More recently, the free energy concentration expansion method (FCEM), which is more accurate than the BW method by including short-range order,¹ has proven to be effective in computations of temperature and concentrations dependent multilayer surface segregation, and in providing insight into the interplay of surface segregation and atomic order in alloys.^{25–27} Obviously, the accuracy of the predictions depends significantly on the reliability of the input energetics. Compared to rather simplified empirical bond energetics used in previous FCEM computations, the present work incorporates homoatomic bond energies and their surface-induced variations, as obtained recently by the Naval Research Laboratory tight-binding method (NRL-TB).^{28,29} This *spd* tight-binding method uses a nonorthogonal TB Hamiltonian, which turns out to be crucial for determining surface energies.^{14,30,31} Interlayer surface relaxation and energy for low-index faces of Rh, Pt, and some other transition metals obtained using the NRL-TB method are in a good agreement when compared to DFT or experiment.²⁸ The present version of the FCEM/TB method is formulated as a tool for the prediction of temperature dependent layer compositions, while elemental surface relaxations enter implicitly via the TB bond energetics.

Most recently, site compositions and thermodynamic properties of Pd-Cu, Rh-Pd, and Rh-Pd-Cu nanoclusters were computed by the same FCEM/TB approach, highlighting the role of surface induced bond energy variations in segregation and ordering phenomena.¹⁶ In view of the lack of relevant experimental data concerning such cluster properties, it is desirable to test this approach in the case of common flat surfaces. Segregation to clean Pt₂₅Rh₇₅(111) surface was chosen for modeling because of the availability of reliable, layer-by-layer experimental data,^{32,33} and results of

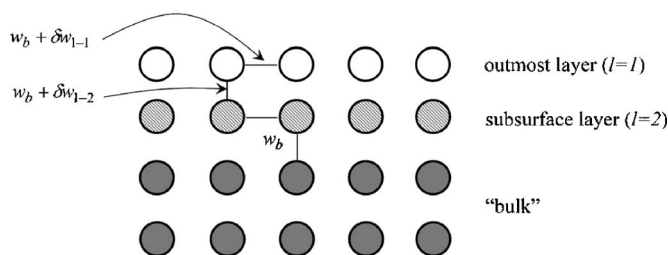


FIG. 1. Illustration of surface induced NN bond energy variations. Note that w is always negative, whereas δw can be either negative (bond strengthening) or positive (bond weakening). The present two-layer model is based on tight-binding data²⁸ for δw_{1-1} and δw_{1-2} (assuming negligible intrasubsurface layer and deeper layer bond variations).

comparative first-principle calculations.^{34–36} A small atomic size mismatch ($\sim 3\%$) and the important role of subsurface tension effects in this alloy system are additional reasons for the choice. The following part clarifies relations between bond energy variations and layer tensions, as well as their effects on surface segregation.

Formulation and energetics

The surface energy of a solid containing N atoms is given by

$$E_s = E - E_b(N), \quad (1)$$

where E is the total energy of the system and $E_b(N)$ is the energy associated with equivalent number of bulk atoms. In the nearest neighbor (NN) pair interaction model the surface energy of elemental solid (I) can be expressed by a sum of atomic site related contributions

$$E_s^I = \sum_m \frac{1}{2} \left(\sum_n^{(m)} w_{mn}^{II} - z_b w_b^{II} \right) = \sum_m \frac{1}{2} \left(\sum_n^{(m)} \delta w_{mn}^{II} - \Delta z_m w_b^{II} \right), \quad (2)$$

where $\sum_n^{(m)}$ goes over the NN of site m , $\delta w_{mn}^{II} = w_{mn}^{II} - w_b^{II}$ denotes the variation in the energy of bonding between sites m and n relative to the bulk value (Fig. 1), z_b and Δz_m denote the bulk coordination number and the number of broken bonds for site m , respectively. As is quite common in the segregation literature^{2,37} the term “tension” is used below instead of “energy” (although strictly speaking the two terms may differ somewhat for solid surfaces). It is convenient to define “ m -site tension,” γ_m^I , “ l -layer tension,” γ_l^I , and “total surface tension,” γ_{tot}^I , according to

$$E_s^I = \sum_m \gamma_m^I = N_{layer} \sum_l \gamma_l^I = N_{layer} \gamma_{tot}^I, \quad (3)$$

where N_{layer} is the number of atoms per layer.

It follows from Eqs. (2) and (3) that if subsurface sites have no broken bonds, e.g., below the low index fcc(111) and (100) surfaces, the corresponding tensions stem only from alteration of the subsurface bonds, and are negative if they strengthen ($\delta w_{mn}^{II} < 0$). If subsurface bonds do not alter, γ_{tot}^I coincides with the outermost layer tension, γ_1^I .

The present computations employ the full FCEM formula²⁷ for the alloy free energy, F , that contains energy and entropy contributions. The former contribution comprises homoatomic interactions and mixing energy (including short-range order), that is related to the effective heteroatomic interactions, $V_{mn}^{IJ} = \frac{1}{2}(w_{mn}^{II} + w_{mn}^{JJ} - 2w_{mn}^{IJ})$. The V_{mn}^{Pt-Rh} value is relatively small, so the major energetic contribution is expected to originate from homoatomic interactions. Therefore, it is justified to focus first on this contribution

$$\tilde{F} = \sum_m \sum_I c_m^I \left(\frac{1}{2} \sum_n^{(m)} w_{mn}^{II} \right), \quad (4)$$

where c_m^I denotes the concentration of constituent I at site m . \tilde{F} can be expressed by means of site or layer tensions defined above

$$\begin{aligned} \tilde{F} &= \sum_m \sum_{I(I \neq S)} (\gamma_m^I - \gamma_m^S) c_m^I = \sum_m \sum_{I(I \neq S)} \Delta \gamma_m^{I-S} c_m^I \\ &= N_{layer} \sum_l \sum_{I(I \neq S)} \Delta \gamma_l^{I-S} c_l^I, \end{aligned} \quad (5)$$

where S denotes a reference alloy constituent (e.g., the solvent).

Within the NRL-TB formalism, the total energy of the elemental system is decomposed into effective bond energies between NN atoms according to Eq. (2) of Ref. 28. In the present approach, these energies are employed as the w_{mn}^{II} values in Eqs. (4) and (5), affecting the alloy surface and subsurface tensions. As noted above, the combination of first-principle computations of alloy structure energies with the cluster expansion method was applied in studies of segregation and relaxation in the $\text{Pt}_{25}\text{Rh}_{75}(111)$ surface.^{34–36} While results similar to those described below were obtained, no straightforward explanation of segregation profiles by means of elemental bond energies is possible. The present approach, on the other hand, provides some extra physical insight and relates the “on-site” terms entering the cluster expansion^{35,36} to TB-computed surface induced variations of bond energies in elemental solids, contributing to layer tensions in formula (5). In particular, as explained below, the subsurface will be enriched by the element that exhibits a higher subsurface bond strengthening (namely, lower subsurface tension). The neglect of alloying effects on homoatomic bond energies, was verified for transition metals by electronic structure calculations,³⁸ and is possible when higher order effective interactions (triplets, etc.) are relatively small.³⁹

While constituent surface tension differences are known for a long time among the main factors controlling surface segregation in alloys,^{2,38} much less attention was paid to effects of subsurface tensions, often considered negligible.^{37,38} Segregation oscillations were commonly attributed to the mixing tendency.¹ In the case of Pt-Rh, however, oscillatory profiles were explained by values of the on-site terms,^{35,36} and a similar conclusion can be deduced from computation results of Ref. 34. The role of subsurface tensions was highlighted only in the case of oscillations predicted for Mo-W (with weak demixing tendency),^{40,41} but it was not verified

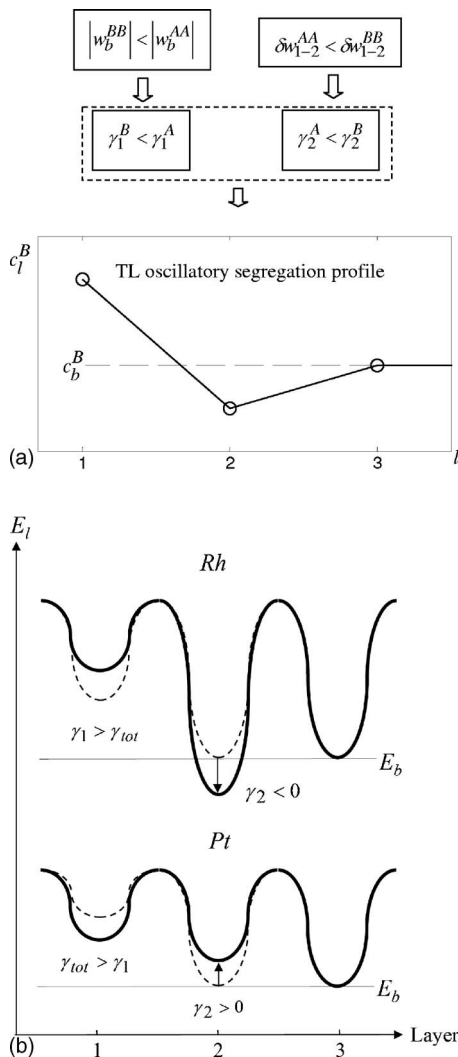


FIG. 2. (a) Schematics of the energetic conditions for two-layer (TL) oscillatory segregation at low index surfaces driven by subsurface tensions. (b) Schematics of Rh(111) and Pt(111) elemental energetics in the two-layer (TL) tension model (solid lines, γ_1 , γ_2 , γ_{tot}). Dashed lines depict the single-layer (SL) tension model.

experimentally. In the present work, predictions of oscillatory segregation driven by subsurface tensions are compared in the next section to experimental data of highly sensitive methods, LEED and MEIS, providing layer-by-layer compositions.^{32,33} As expected from considerations related to charge transfer from broken bonds, NRL-TB data for Ni, Cu, Rh, and Pd, show that typically (but not in case of Pt) transition metal subsurface bonds strengthen²⁸ (bonding between

layers 1–2, Fig. 1; since in the present case all layer sites are equivalent, in the following all numerical subscripts denote atomic layers). Therefore, the corresponding low index subsurface tensions are negative, opposite to the outmost layer surface tensions. Figure 2(a) illustrates the anticipated occurrence of an oscillatory segregation profile in a binary alloy depending on the constituent bond energies and their relative variations. In particular, as can be inferred from Eq. (5), if the subsurface tension of the segregating element is much higher than that of the other constituent, a pronounced oscillation is expected even in case of weak mixing tendency, as discussed in the present study for Pt-Rh, or even in the case of weak demixing tendency, as was predicted for Mo-W mentioned above.^{40,41} Weakening of Pt subsurface bonds compared to strengthening in many other transition metals, is indicated indirectly by experimental LEED measurements and calculated data for separations of the top two layers.²⁸ Hence, significant effects of subsurface tensions on subsurface compositions are expected for Pt alloys in general, although they can somewhat be obscured by mixing or demixing tendency. In the Pt-Rh case the effect becomes most evident, due to the very weak mixing tendency. (Other candidates having relatively small V include Pt-Pd, Pt-Au, and Pt-Ru, but even Pd-Cu with moderate mixing tendency is still expected to exhibit a significant subsurface tension contribution to the Cu oscillatory segregation.¹⁶) According to Eqs. (2) and (3) the pure Rh 1–2 interlayer bond strengthening and Pt bond weakening (Table I) result in a negative (positive) Rh (Pt) subsurface tension [Fig. 2(b)]. Thus, the subsurface tension difference, $\Delta\gamma_2^{\text{Pt-Rh}}$, is positive, resulting in Pt subsurface depletion. On the other hand, the difference of the outmost layer tensions, $\Delta\gamma_1^{\text{Pt-Rh}}$, is negative, leading to Pt enrichment, so that an oscillatory Pt segregation profile is anticipated. Such bonding variation related energetic effects are beyond the scope of simplified models based on empirical site energies⁴² or on scaling of pair interactions as the inverse square root of coordination.⁴³ As can be seen from Table I, layer tension differences based on the present TB data have the same signs as layer-dependent segregation energies of Pt, E_{segr-1}^{Pt} and E_{segr-2}^{Pt} , computed in Ref. 34, but are larger.

Computation results vs experiment

It is instructive to compare two models of surface layer energetics and to apply them to Pt-Rh:

(i) “Single surface layer tension model” (SL) using TB computed total surface tension, but arbitrarily relating it to the outmost layer only. It was employed in some theoretical

TABLE I. NRL-TB computed variations in Pt and Rh bond energies at the (111) surface relative to the bulk values (based on Ref. 29 data) and the corresponding Pt-Rh tension differences (meV). Values of layer-dependent segregation energies of Pt computed in Ref. 34 by DFT-based cluster expansion are shown for comparison.

Element	δw_{1-1}	δw_{1-2}	$\Delta\gamma_1^{\text{Pt-Rh}}$	$\Delta\gamma_2^{\text{Pt-Rh}}$	$\Delta\gamma_{tot}^{\text{Pt-Rh}}$	E_{segr-1}^{Pt}	E_{segr-2}^{Pt}
Pt	-156	+60	-490	+140	-350	-281	+85
Rh	-52	-32					

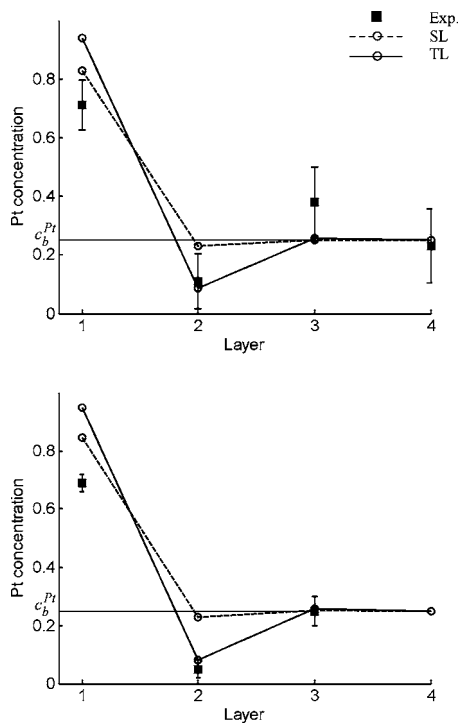


FIG. 3. FCEM/TB computed surface segregation profiles for $\text{Pt}_{25}\text{Rh}_{75}(111)$ vs experimental data (black squares) of LEED (Ref. 32) at 1373 K (upper panel), and of MEIS (Ref. 33) at 1300 K (lower panel). Solid lines—the two layer tension model (TL); dashed lines—the single layer tension model (SL).

studies neglecting contributions of deeper layer tensions.^{37,38}

(ii) The “two layer tension model” (TL) presented here, using TB computed outmost and subsurface layer tensions.

Segregation profiles, based on the two models and computed by FCEM using the NRL-TB bond energies, are shown in Fig. 3 together with LEED data³² at 1373 K and MEIS data³³ at 1300 K. According to the TL model compared to the SL model, even at these high temperatures two distinct phenomena are exhibited by the outmost two layers (deeper layer compositions remain nearly unchanged): (i) Oscillatory Pt segregation profile (subsurface layer depletion), and (ii) Extra Pt segregation at the outmost layer. As mentioned above, the common origin of oscillatory surface segregation does not apply to the Pt-Rh case, since the mixing tendency in this alloy is very weak in the bulk⁴⁴ and at the surface.^{35,45} In particular, using formation enthalpy calculated by means of the linearized augmented plane-wave method,⁴⁶ the heteroatomic effective interactions, included in the FCEM input energetics, are estimated as $V \approx 4$ meV only. However, due to the quite appreciable value of $\Delta\gamma_2^{\text{Pt-Rh}}$ (Table I), the subsurface oscillation persists up to quite high temperatures, as obtained experimentally.

The origin of the outmost layer extra Pt segregation in the TL model is simply related to $|\Delta\gamma_1^{\text{Pt-Rh}}|$ being larger than $|\Delta\gamma_{\text{tot}}^{\text{Pt-Rh}}|$, since $\gamma_{\text{tot}}^{\text{Rh}} < \gamma_1^{\text{Rh}}$ and $\gamma_{\text{tot}}^{\text{Pt}} > \gamma_1^{\text{Pt}}$ [Fig. 2(b)]. Although we refer to concentrations of the two outmost layers equilibrated at two temperatures only, comparison of the computation results with the MEIS and LEED data clearly shows

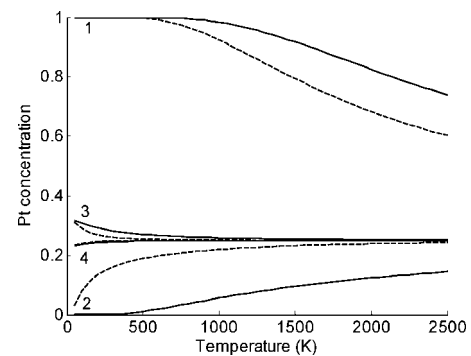


FIG. 4. The FCEM/TB computed temperature dependence of near surface layer concentrations (indicated by numbers) in $\text{Pt}_{25}\text{Rh}_{75}(111)$. TL model—solid lines; SL model—dashed lines.

that the TL model oscillation is more accurate than in the SL model. Thus, the incorporation of the outmost and subsurface layer tensions via NRL-TB data of bond energy variations, yields the observed trends, namely, enrichment of Pt at the outmost layer coupled with its significant depletion in the subsurface layer, without any adjustable parameters and in agreement with the predictions of Refs. 34 and 35.

The thermal evolution of the oscillatory layer concentrations computed for $\text{Pt}_{25}\text{Rh}_{75}(111)$ is shown in Fig. 4. Driven by the underlying energetics, pure Pt surface layer and pure Rh subsurface layer emerge at low temperatures. With temperature increase, the oscillations gradually decrease by entropy driven mixing. Since V is small, compositional oscillations in deeper layers (third and fourth) are much weaker than the subsurface oscillation (second layer) stemming from the surface-subsurface bond variations. In the SL model ignoring these variations, the subsurface oscillation due to V only is much weaker than in the TL model at all temperatures (Figs. 3 and 4).

In conclusion, effects of surface induced homoatomic bond energy variations on surface and subsurface segregation in alloys are elucidated theoretically and demonstrated for $\text{Pt}_{25}\text{Rh}_{75}(111)$ as a test case. In case of opposite sign of the differences in the outmost vs. subsurface layer constituent tensions, significant oscillatory surface segregation can arise even in alloys with a weak mixing tendency as Pt-Rh, or even in weak demixing alloys. Key ingredients in the proposed approach are input energetics based on NRL-TB data that are used in conjunction with the FCEM statistical-mechanical approximation in order to account also for the configurational entropy and finite-temperature properties. The high transparency of this approach furnishes physical understanding of the relatively unfamiliar origin of oscillatory segregation profiles. Reasonable agreement with the available experimental data is obtained only for the two layer tension model, indicating the potential validity of the FCEM/TB approach, which can be extended, e.g., to model computations of site composition related properties of alloy nanoclusters.¹⁶ However, for higher accuracy further refinement of the input energetics entering FCEM is needed, such

as taking into account on-site TB integrals, which might contribute to site tensions beyond (improved) pair bond energies. Likewise, studies of alloy systems having considerable mixing or demixing tendencies and/or atomic size mismatch should include TB computed heteroatomic bond energies in different coordinations and alloy lattice relaxations. Furthermore, computations of bond energies beyond the NN contributions are planned, possibly affecting also the compositions of deeper layers. Yet, even in its present state, the FCEM/TB

approach can adequately account for certain aspects of surface segregation in alloys.

ACKNOWLEDGMENTS

We wish to thank M. I. Haftel and N. Bernstein (Center for Computational Materials Science, Naval Research Laboratory, Washington, DC) for providing us with the NRL-TB data. This research was supported by The Israel Science Foundation (Grant No. 1204/04).

*Author to whom correspondence should be addressed. Electronic address: mpolak@bgu.ac.il

- ¹M. Polak and L. Rubinovich, *Surf. Sci. Rep.* **38**, 127 (2000).
- ²P. Wynblatt and R. C. Ku, *Surf. Sci.* **65**, 511 (1977).
- ³A. V. Ruban, H. L. Skriver, and J. K. Norskov, *Phys. Rev. B* **59**, 15990 (1999).
- ⁴S. M. Foiles, in *Surface Segregation Phenomena*, edited by P. A. Dowben and A. Miller (CRC Press, Boca Raton, Florida, 1990), pp. 79–106.
- ⁵M. S. Daw and M. I. Baskes, *Phys. Rev. B* **29**, 6443 (1984).
- ⁶Z.-J. Tian and T. S. Rahman, *Phys. Rev. B* **47**, 9751 (1993).
- ⁷K. W. Jacobsen, J. K. Norskov, and M. J. Puska, *Phys. Rev. B* **35**, 7423 (1987).
- ⁸K. W. Jacobsen, P. Stoltze, and J. K. Norskov, *Surf. Sci.* **366**, 394 (1996).
- ⁹G. Treglia, B. Legrand, F. Ducastelle, A. Saul, C. Gallis, I. Meunier, C. Mottet, and A. Senhaji, *Comput. Mater. Sci.* **15**, 196 (1999).
- ¹⁰C. Mottet, G. Treglia, and B. Legrand, *Phys. Rev. B* **66**, 045413 (2002).
- ¹¹S. Mukherjee and J. L. Moran-Lopez, *Surf. Sci.* **188**, L742 (1987).
- ¹²M. C. Desjonqueres and D. Spanjaard, *Phys. Rev. B* **35**, 952 (1987).
- ¹³S. Papadía, M. C. Desjonquères, and D. Spanjaard, *Phys. Rev. B* **53**, 4083 (1996).
- ¹⁴M. J. Mehl and D. A. Papaconstantopoulos, *Phys. Rev. B* **54**, 4519 (1996).
- ¹⁵S. Baud, C. Ramseyer, G. Bihlmayer, S. Blügel, C. Barreateau, M. C. Desjonquères, D. Spanjaard, and N. Bernstein, *Phys. Rev. B* **70**, 235423 (2004).
- ¹⁶L. Rubinovich, M. I. Haftel, N. Bernstein, and M. Polak, *Phys. Rev. B* **74**, 035405 (2006).
- ¹⁷F. L. Williams and D. Nason, *Surf. Sci.* **45**, 377 (1974).
- ¹⁸J. L. Moran-Lopez and K. H. Bennemann, *Phys. Rev. B* **15**, 4769 (1977).
- ¹⁹A. Jablonsky, *Adv. Colloid Interface Sci.* **8**, 213 (1977).
- ²⁰J. L. Moran-Lopez and L. M. Falicov, *Phys. Rev. B* **18**, 2542 (1978).
- ²¹J. L. Moran-Lopez and L. M. Falicov, *Phys. Rev. B* **18**, 2549 (1978).
- ²²V. Kumar and K. H. Bennemann, *Phys. Rev. Lett.* **53**, 278 (1984).
- ²³J. M. Sanchez and J. L. Moran-Lopez, *Phys. Rev. B* **32**, 3534 (1985).
- ²⁴A. V. Ruban, I. A. Abrikosov, D. Ya. Kats, D. Gorelikov, K. W. Jacobsen, and H. L. Skriver, *Phys. Rev. B* **49**, 11383 (1994).
- ²⁵J. M. Roussel, A. Saul, L. Rubinovich, and M. Polak, *J. Phys.: Condens. Matter* **11**, 9901 (1999).
- ²⁶M. Polak, C. S. Fadley, and L. Rubinovich, *Phys. Rev. B* **65**, 205404 (2002).
- ²⁷L. Rubinovich and M. Polak, *Surf. Sci.* **513**, 119 (2002).
- ²⁸M. I. Haftel, N. Bernstein, M. J. Mehl, and D. A. Papaconstantopoulos, *Phys. Rev. B* **70**, 125419 (2004).
- ²⁹M. I. Haftel (private communication).
- ³⁰R. E. Cohen, M. J. Mehl, and D. A. Papaconstantopoulos, *Phys. Rev. B* **50**, 14694 (1994).
- ³¹D. A. Papaconstantopoulos and M. J. Mehl, *J. Phys.: Condens. Matter* **15**, R413 (2003).
- ³²E. Platzgummer, M. Sporn, R. Koller, S. Forsthuber, M. Schmid, W. Hofer, and P. Varga, *Surf. Sci.* **419**, 236 (1999).
- ³³D. Brown, P. D. Quinn, D. P. Woodruff, T. C. Q. Noakes, and P. Bailey, *Surf. Sci.* **497**, 1 (2002).
- ³⁴A. V. Ruban and H. L. Skriver, *Comput. Mater. Sci.* **15**, 119 (1999).
- ³⁵S. Muller, M. Stohr, and O. Wieckhorst, *Appl. Phys. A* **82**, 415 (2006).
- ³⁶V. Drchal, A. Pasturel, R. Monnier, J. Kudrnovsky, and P. Weinberger, *Comput. Mater. Sci.* **15**, 144 (1999).
- ³⁷F. Ducastelle, B. Legrand, and G. Treglia, *Prog. Theor. Phys. Suppl.* **101**, 159 (1990).
- ³⁸G. Treglia, B. Legrand, and F. Ducastelle, *Europhys. Lett.* **7**, 575 (1988).
- ³⁹S. Ouannasser, L. T. Wille, and H. Dreysse, *Phys. Rev. B* **55**, 14245 (1997).
- ⁴⁰S. Ouannasser, H. Dreysse, and L. T. Wille, *Solid State Commun.* **96**, 177 (1995).
- ⁴¹S. Ouannasser, L. T. Wille, and H. Dreysse, *Surf. Sci.* **553**, 30 (2004).
- ⁴²Ling Zhu and Andrew E. DePristo, *J. Catal.* **167**, 400 (1997).
- ⁴³M. Methfessel, D. Hennig, and M. Scheffler, *Appl. Phys. A: Solids Surf.* **55**, 442 (1992).
- ⁴⁴Ch. Steiner, B. Schönfeld, M. J. Portmann, M. Kompatscher, G. Kostorz, A. Mazuelas, T. Metzger, J. Kohlbrecher, and B. Deme, *Phys. Rev. B* **71**, 104204 (2005).
- ⁴⁵E. L. D. Hebenstreit, W. Hebenstreit, M. Schmid, and P. Varga, *Surf. Sci.* **441**, 441 (1999).
- ⁴⁶Z. W. Lu, S.-H. Wei, and Alex Zunger, *Phys. Rev. Lett.* **66**, 1753 (1991).